

SUPPLEMENTARY INFORMATION

A novel double kink-turn module in euryarchaeal RNase P RNAs

Lien B. Lai,^{1,2,*} Akiko Tanimoto,^{1,#} Stella M. Lai,^{1,2,#}

Wen-Yi Chen,^{1,2,+} Ila A. Marathe,¹⁻³

Eric Westhof⁴, Vicki H. Wysocki¹ and Venkat Gopalan^{1-3,*}

¹Department of Chemistry & Biochemistry,

²Center for RNA Biology,

³Department of Microbiology,

The Ohio State University, Columbus, OH 43210, USA

⁴Institut de Biologie Moléculaire et Cellulaire

Centre National de la Recherche Scientifique

67084 Strasbourg Cedex, FRANCE

+ Current address: Nexcelcom Bioscience, San Diego, CA 92121

These authors contributed equally to this work.

* To whom correspondence should be addressed. Tel: 1-614-292-1331; Fax: 1-614-292-6773; Email: gopalan.5@osu.edu. Correspondence may also be addressed to Lien B. Lai. Tel: 1-614-292-2036; Fax: 1-614-292-6773; Email: lai.104@osu.edu.

SUPPLEMENTARY TEXT

Mutagenesis, in vitro transcription, and refolding of RNAs

PfuRPR, MjaRPR and MmaRPR were cloned previously in our laboratory (1-4). PCR-based mutagenesis of PfuRPR and MjaRPR was used to change the sheared GA to GC base pairs at each K-turn individually and in combination. We also describe below the cloning of gel-shift PfuRPR fragments.

PfuRPR-mKT1 and all three MjaRPR mutants: The 5'-phosphorylated mutagenic primers (Supplementary Table S1) were designed to anneal back-to-back and to amplify the whole template plasmid (either pBT7-PfuRPR or pBT7-MjaRPR). The amplicons were then ligated to recircularize before transforming DH5 α .

PfuRPR-mKT2, -mKT3, and -mKT23: The mutagenic primers were used to amplify the fragment containing nucleotides 129-197, and PfuP12-F and -R (both 5'-phosphorylated) were used to amplify the remainder of pBT7-PfuRPR. These two fragments were then ligated before transforming DH5 α , and colonies were screened for transformants containing a correctly oriented insert.

PfuRPR-mKT123: Overlapping PCR of fragment 1 (amplified using template pBT7-PfuRPR-mKT23 and primers F-ext and PfuRPRp5/16-R) and fragment 2 (amplified using template pBT7-PfuRPR-mKT1 and primers R-ext and PfuRPRmKT123-F) was used to create PfuRPR-mKT123 with flanking vector sequences. Subsequent to digestion with BssHII, the insert was ligated into BssHII-digested pBT7 for cloning.

Gel-shift fragments of PfuRPR (gsPfuP12): These fragments were cloned by PCR-based fill-in of overlapping primers and subsequent insertion into Stu-digested pBT7.

All mutagenized clones were confirmed by automated DNA sequencing. The clones were then used as templates in PCRs to generate *in vitro* transcription (IVT) templates with the primers F-ext and R-ext (Supplementary Table S1); each PCR product was then digested with appropriate restriction enzymes to facilitate run-off IVT as described elsewhere (PfuRPR and MmaRPR with EcoRI; MjaRPR with BsmAI; gsPfuP12 with SmaI) (1-4).

The transcribed RPRs were then refolded for MS (5) and footprinting experiments (6), as well as for RNase P assays (1-4). Each RPR was incubated in water for 50 min at 50°C and 10 min at 37°C, and an equal volume of 2x folding buffer was added before incubating for 30 min at 37°C. The 2x folding buffer had 1.6 M NH₄OAc and 20 mM MgCl₂; for footprinting experiments and RNase P assays, it also had 50 mM HEPES, pH 8 (at 22°C).

Purification of recombinant *Pfu*, *Mja*, and *Mma* L7Ae

PfuL7Ae and its single cysteine derivatives (PfuL7Ae-K42C and -V95C) were purified, and the single-Cys derivatives were modified with EDTA-2-aminoethyl 2-pyridyl disulfide (EPD; Toronto Research Chemicals) to covalently attach the EDTA-Fe moiety using methods described before (6).

His₆-MjaL7Ae, overexpressed from a pET-28a clone that was kindly provided by Dr. E. Stuart Maxwell (North Carolina State University, Raleigh, NC), was first purified using a 1-mL HisTrap HP column (GE Healthcare) as described elsewhere (7). The fractions enriched for L7Ae were then pooled and solid NaCl was added to obtain a final

concentration of 3 M. The sample was then passed through a 1-mL HiTrap Phenyl Sepharose HP column (GE Healthcare) to capture contaminating proteins and leave His₆-MjaL7Ae in the flow-through. To remove the His₆ affinity tag, the flow-through was dialyzed against a thrombin cleavage buffer [20 mM Tris-HCl (pH 8), 150 mM NaCl, 2.5 mM CaCl₂] and treated with biotinylated thrombin (EMD Millipore). While the biotinylated thrombin was subsequently removed by treating with magnetic streptavidin beads (Bioclone), the cleaved His₆-tag was captured using Ni-NTA resin (Roche Diagnostics). MjaL7Ae was dialyzed against water to decrease salt content, loaded onto a C4 semi-preparative reversed-phase column (250 x 10 mm; Higgins Analytical), and eluted at 3 mL/min with solvent A (99.9% water, 0.1% TFA) and solvent B (99.9% acetonitrile, 0.1% TFA) using the following program: 5% B for 10 min, a linear gradient of 5-95% B for 60 min, and 95% B for 5 min. MjaL7Ae eluted between 58-60% acetonitrile. Individual peak fractions were lyophilized then resuspended in buffer R [10 mM sodium phosphate (pH 6.5), 6 M guanidine hydrochloride]. Absorbance at 260 and 280 nm was measured, and only the fractions with A_{260}/A_{280} of 0.5–0.6 (reflective of low nucleic acid content) were pooled. MjaL7Ae was refolded by increasing the volume to 15 mL with buffer R and dialyzing overnight against 3 L of buffer M [10 mM Tris-HCl (pH 8), 10 mM KCl, 5 mM DTT], followed by 3 L of buffer F [10 mM Tris-HCl (pH 8)]. This preparation was then concentrated using an Amicon Ultra-15 Centrifugal Filter unit (3,000 MWCO; Millipore), and the final concentration was estimated using $\epsilon = 5240 \text{ M}^{-1}\text{cm}^{-1}$ and the measured A_{280} value.

MmaL7Ae was first purified using Q- and phenyl-Sepharose sequentially (4). After dialyzing against 20 mM Tris-HCl (pH 7.5), MmaL7Ae was loaded on a reversed-phase C4 analytical column (150 x 4.6 mm; Grace Vydac) and eluted at 0.9 mL/min with solvent A (99.9% water, 0.1% TFA) and solvent B (90% acetonitrile, 0.1% TFA) in the following program: 5% B for 5 min, a linear gradient from 5-95% B for 30 min, and 95% B for 2.5 min. MmaL7Ae eluted between 72-85% acetonitrile. Individual peak fractions were lyophilized then resuspended in buffer R. Absorbance at 260 and 280 nm was measured, and only the fractions with A_{260}/A_{280} of ~ 0.7 were pooled. MmaL7Ae was refolded by increasing the volume to 15 mL with buffer R and dialyzing overnight against 3 L of buffer M, followed by 3 L of buffer F. BCA assay with BSA as a reference standard was used to determine the concentration of MmaL7Ae. Prior to MS experiments, MmaL7Ae was incubated with 10 mM TCEP at 25°C for 15 min to minimize disulfide-mediated dimerization before dialyzing against 10 mM ammonium acetate for 12 - 16 h at 4°C.

Gel-shift analyses

To fold the *Pfu* P12 fragments (WT, mKT2, and mKT3), a trace amount of 5'-³²P-labeled RNA (1.25×10^5 dpm) was incubated with an equal volume of 2x folding buffer [100 mM HEPES-KOH (pH 8 at 22°C), 1.6 M NH₄OAc, 20 mM MgCl₂] for 2 min at 100°C and then slowly cooled to room temperature. An equal volume of L7Ae in 1x folding buffer supplemented with 20% (v/v) glycerol was then added to each RNA sample to achieve the desired final L7Ae concentration (0, 10, 100, 1,000, or 10,000 nM). Each reaction

was subsequently incubated for 10 min at 37°C, placed on ice, and electrophoresed on a pre-run (35 mA for 90 min at 4°C) 8% (w/v) polyacrylamide (19:1) native gel at 35 mA for 3 h at 4°C. The running buffer contained 50 mM HEPES-KOH (pH 8 at 22°C), 1 mM Mg(OAc)₂, and 0.01% IGEPAL CA-630 (Sigma-Aldrich). Reaction products were visualized with a Typhoon phosphorimager (GE Healthcare), and ImageQuant (GE Healthcare) was used to assess the extent of complex formation.

RNase P assays

RNase P assays were performed as described by us before (1-4) using *Escherichia coli* pre-tRNA^{Tyr} as the substrate, a trace amount of which was labeled with [α -³²P] GTP. All reconstitutions and assays were performed in a thermal cycler to ensure accurate control of the assay temperature. PfuRPR was freshly folded before each use. For comparing the multiple-turnover activities of the holoenzyme with four RPPs (10 nM Pfu RPR + 100 nM POP5•RPP30 +100 nM RPP21•RPP29) or five RPPs (10 nM Pfu RPR + 100 nM POP5•RPP30 +100 nM RPP21•RPP29 + 100 nM L7Ae), the respective RNPs were assembled by incubation at 55°C for 10 min in 50mM HEPES (pH 8 at 22°C), 800mM NH₄OAc and the indicated concentrations of MgCl₂ before addition of 500nM pre-tRNA^{Tyr} pre-warmed at 55°C in the same buffer as the holoenzyme. Reactions were performed at 55°C, and aliquots were removed at defined time intervals for determination of turnover number. The aliquots withdrawn were quickly added to an equal volume of stop solution [10M urea, 5mM EDTA, 0.05% (w/v) bromophenol blue, 0.05% (w/v) xylene cyanol, 10% (v/v) phenol] to terminate the

reaction. The reaction contents were separated using denaturing PAGE [8% (w/v) polyacrylamide, 7 M urea] and visualized using a phosphorimager (Typhoon, GE Healthcare). The ImageQuant (GE Healthcare) software was used to determine product formation as a function of time.

REFERENCES

1. Tsai, H.Y., Pulukkunat, D.K., Woznick, W.K. and Gopalan, V. (2006) Functional reconstitution and characterization of *Pyrococcus furiosus* RNase P. *Proc. Natl. Acad. Sci. USA*, **103**, 16147-16152.
2. Pulukkunat, D.K. and Gopalan, V. (2008) Studies on *Methanocaldococcus jannaschii* RNase P reveal insights into the roles of RNA and protein cofactors in RNase P catalysis. *Nucleic Acids Res.*, **36**, 4172-4180.
3. Chen, W.Y., Pulukkunat, D.K., Cho, I.M., Tsai, H.Y. and Gopalan, V. (2010) Dissecting functional cooperation among protein subunits in archaeal RNase P, a catalytic ribonucleoprotein complex. *Nucleic Acids Res.*, **38**, 8316-8327.
4. Cho, I.M., Lai, L.B., Susanti, D., Mukhopadhyay, B. and Gopalan, V. (2010) Ribosomal protein L7Ae is a subunit of archaeal RNase P. *Proc. Natl. Acad. Sci. USA*, **107**, 14573-14578.
5. Ma, X., Lai, L.B., Lai, S.M., Tanimoto, A., Foster, M.P., Wysocki, V.H. and Gopalan, V. (2014) Uncovering the stoichiometry of *Pyrococcus furiosus* RNase P, a multi-subunit catalytic ribonucleoprotein complex, by surface-induced dissociation and ion mobility mass spectrometry. *Angew. Chem. Int. Ed. Engl.*, **53**, 11483-11487
6. Lai, S.M., Lai, L.B., Foster, M.P. and Gopalan, V. (2014) The L7Ae protein binds to two kink-turns in the *Pyrococcus furiosus* RNase P RNA. *Nucleic Acids Res.*, **42**, 13328-13338.
7. Gagnon, K., Zhang, X. and Maxwell, E.S. (2007) In vitro reconstitution and affinity purification of catalytically active archaeal box C/D sRNP complexes. *Methods Enzymol.*, **425**, 263-282.

8. Meyer, M., Westhof, E. and Masquida, B. (2012) A structural module in RNase P expands the variety of RNA kinks. *RNA Biol.*, **9**, 254-260.
9. Daldrop, P., Masquida, B. and Lilley, D.M.J. (2013) The functional exchangeability of pk- and k-turns in RNA structure. *RNA Biol.*, **10**, 445-452.
10. Reiter, N.J., Osterman, A., Torres-Larios, A., Swinger, K.K., Pan, T. and Mondragon, A. (2010) Structure of a bacterial ribonuclease P holoenzyme in complex with tRNA. *Nature*, **468**, 784-789.

Supplementary Table S1

DNA oligonucleotides used for site-directed mutagenesis of PfuRPR and MjaRPR and for construction of the gel-shift Pfu P12 fragments

Primer	Sequence	Nt #	Clone
PfuKT1-F	GGTGTG <u>CGG</u> CCCGTG	258-272	PfuRPR-mKT1
PfuKT1-R	GGGAACGCATCGGCC	257-242	
PfuKT2-F	GGGGATG <u>CGG</u> ATGAAAGC	129-146	PfuRPR-mKT2
PfuKT2-R	CTCGGGAGCGTCTGCGG	197-181	
PfuKT3-F	GGGGATGTGGATG <u>CAAG</u> CGGTGAAG	129-153	PfuRPR-mKT3
PfuKT3-R	CTCGGGATTGGCTGCGGGTTAA	197-176	
PfuKT23-F	GGGGATG <u>CGG</u> ATG <u>CAAG</u> CGGTGAAG	129-153	PfuRPR-mKT23
PfuKT23-R	CTCGGGAGCGGCTGCGGGTTAA	197-176	
PfuP12-F	GGGAGCGGTGAAACGG	198-213	PfuRPR-mKT2, 3 & 23
PfuP12-R	CGAGGGACGTGTCGTTTC	128-111	
PfuKT123-F	GGGGTGCAAGGCCGAGTTAG	223-242	PfuRPR-mKT123
PfuRPR5/16-R	CTAACTCGGCCTTGAC	242-226	
F-ext	CGACGTTGTAAAACGACGGCCAG	Vector	
R-ext	GGAAACAGCTATGACCATGATTACGCCAAG	Vector	
MjaRPRmKT-F	GGAGAACCGGTGAAACGG	161-178	MjaRPR-mKT2, 3 & 23
MjaRPRmKT2-R	GGAAGGCCTCAACTTTTCACTATCATCGGCATCTCTTCCGGAGCCG	160-116	MjaRPR-mKT2
MjaRPRmKT3-R	GGAAGTCCGCAACTTTTCACTAGCATCGTCATCTCTTCCGGAG	160-119	MjaRPR-mKT3
MjaRPRmKT23-F	GGAAGGCCGCAACTTTTCACTAGCATCGGCATCTCTTCCGGAGCCG	160-116	MjaRPR-mKT23
gsPfuP12-1F	GGGGGATGTGGATGAAAGCGGgaaaCCG	128-148	Pfu P12 WT
gsPfu P12-1R	cccggGGGATTGTCTGCGGtttcCCG	194-181	
gsPfu P12-2F	GGGGGATG <u>CGG</u> ATGAAAGCGGgaaaCCG	128-148	Pfu P12 mKT2
gsPfu P12-2R	cccggGGGAGCGTCTGCGGtttcCCG	194-181	
gsPfu P12-3F	GGGGGATGTGGATG <u>CAAG</u> CGGgaaaCCG	128-148	Pfu P12 mKT3
gsPfu P12-3R	cccggGGGATTGTCTGCGGtttcCCG	194-181	

Notes:

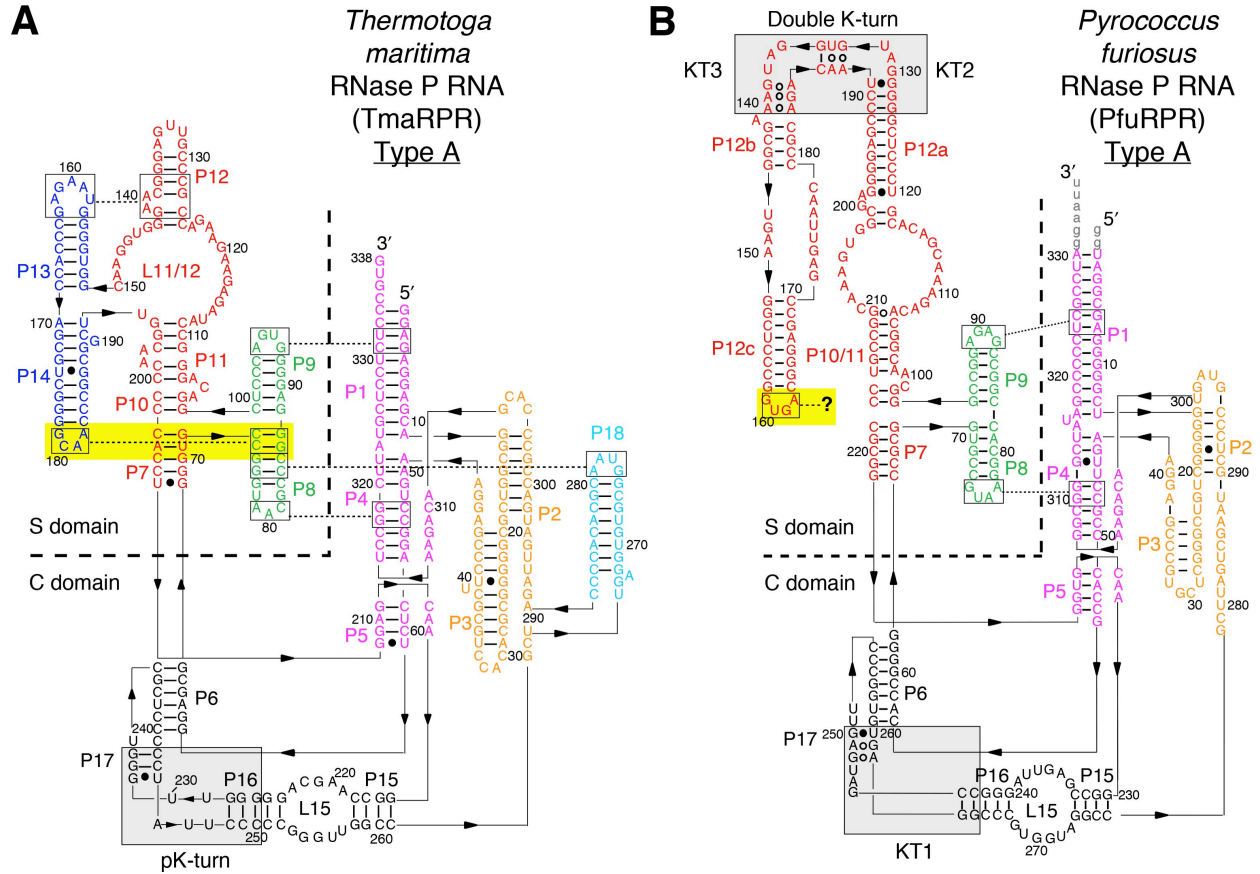
1. Mutagenic nucleotides are underlined.
2. Lowercase nucleotides in the gsPfuKT23 primers: “gaaa” was added to cap the helix with a GNRA tetraloop; “cccgg” was added to complement and strengthen the stem formed by the two termini.
3. Nt #: Nucleotide numbering of the respective RPR to which the primer was designed to anneal (only for the first stretch of uppercase sequence).

Supplementary Table S2

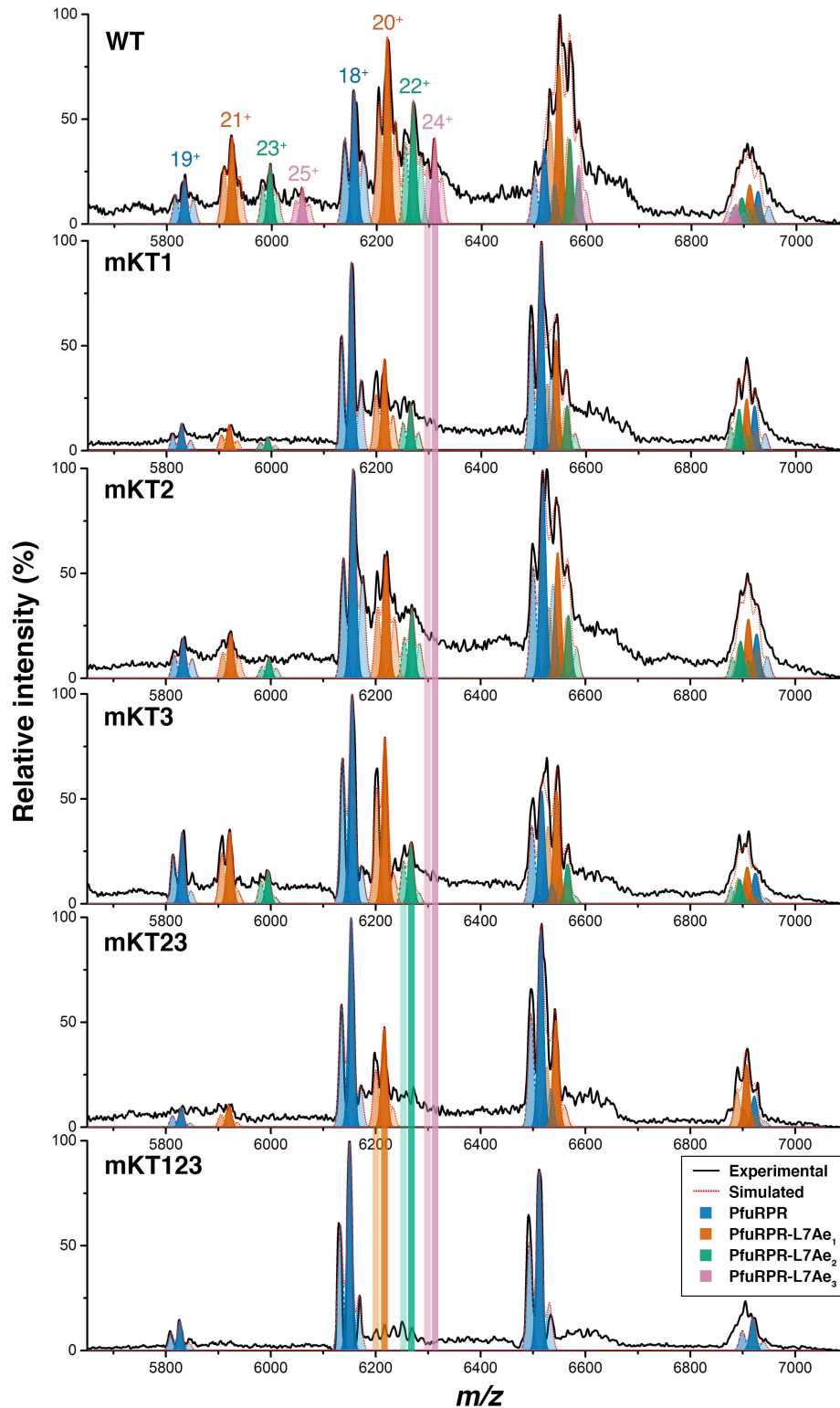
DNA oligonucleotides used for primer extension

Primer	Sequence	Nucleotides in PfuRPR
PfuRPR-2R	GGACGGCCGTTTCACC	227-202
PfuRPRj15/2-R	GGGAGCATTTCGACTAAGC	295-278

SUPPLEMENTARY FIGURES AND LEGENDS



Supplementary Figure S1. Secondary structure of the type A RPRs: **(A)** TmaRPR, bacterial, and **(B)** PfuRPR, archaeal. Note that in P16-17 of both RPRs (gray boxes), there is a kink module called a pK-turn in TmaRPR (8,9) and a K-turn (KT1) in PfuRPR. The double K-turn likely enables P12 fold back in PfuRPR to act as a substitute for the missing P13-14 stack that is present in TmaRPR (10). The tetraloop L12 in PfuRPR could serve like the tetraloop L14 in TmaRPR (both highlighted in yellow), although its receptor remains to be mapped.



Supplementary Figure S2. Native MS spectra of PfuRPR-L7Ae complexes overlaid with Gaussian simulation to aid peak identification. The simulation is a guide to highlight

experimentally observed peaks of free PfuRPR, PfuRPR-L7Ae₁, PfuRPR-L7Ae₂, and PfuRPR-L7Ae₃ as indicated. The simulation was generated using the Gaussian function,

$$f(x) = h \exp\left(-\frac{\left(x - \left(\frac{m + \sigma + z}{z}\right)\right)^2}{\left(\frac{\sqrt{2}}{3z}\sigma\right)^2}\right),$$

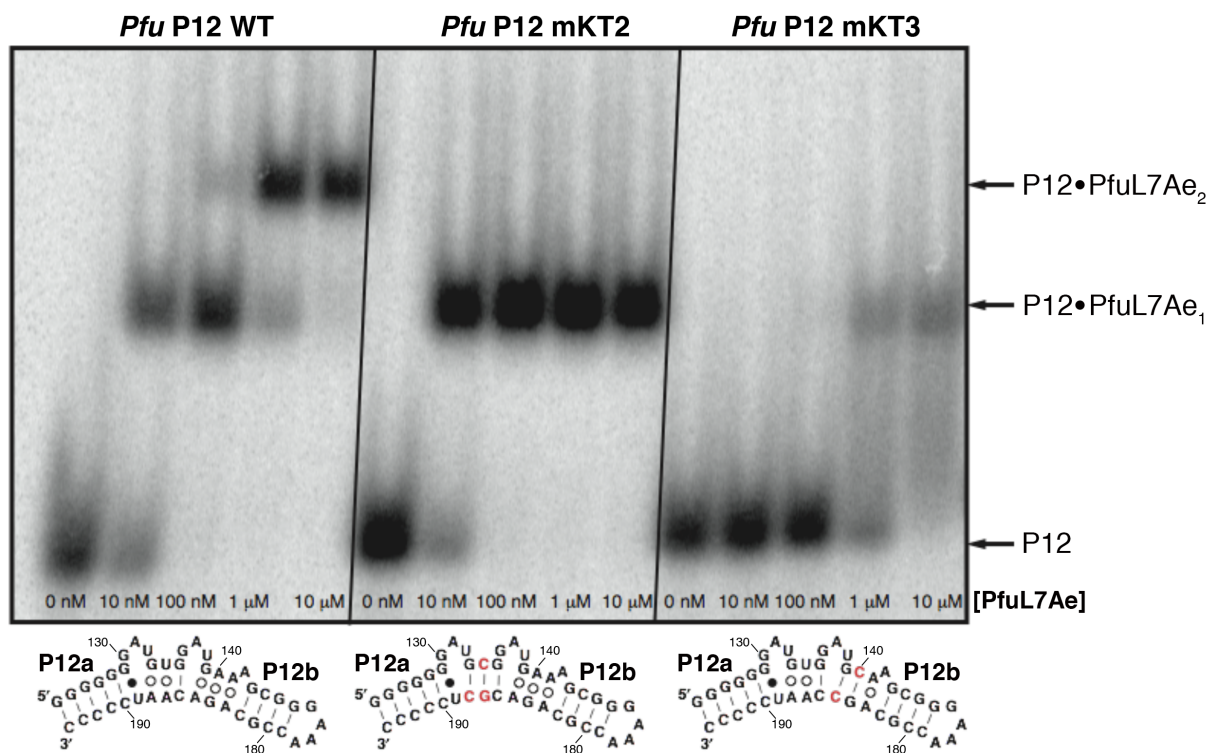
where h is peak height, x is the experimental m/z , m is

theoretical average mass, σ is peak width at the base of the peak, and z is the charge state. Peak width in different analyses vary slightly due to lack of uniformity of the shape and diameter of the capillary tips used for ionization. Therefore, σ was estimated in each analysis to match the observed peak width. h was also adjusted based on the observed peak height. The variables used in the simulation are shown in the table below.

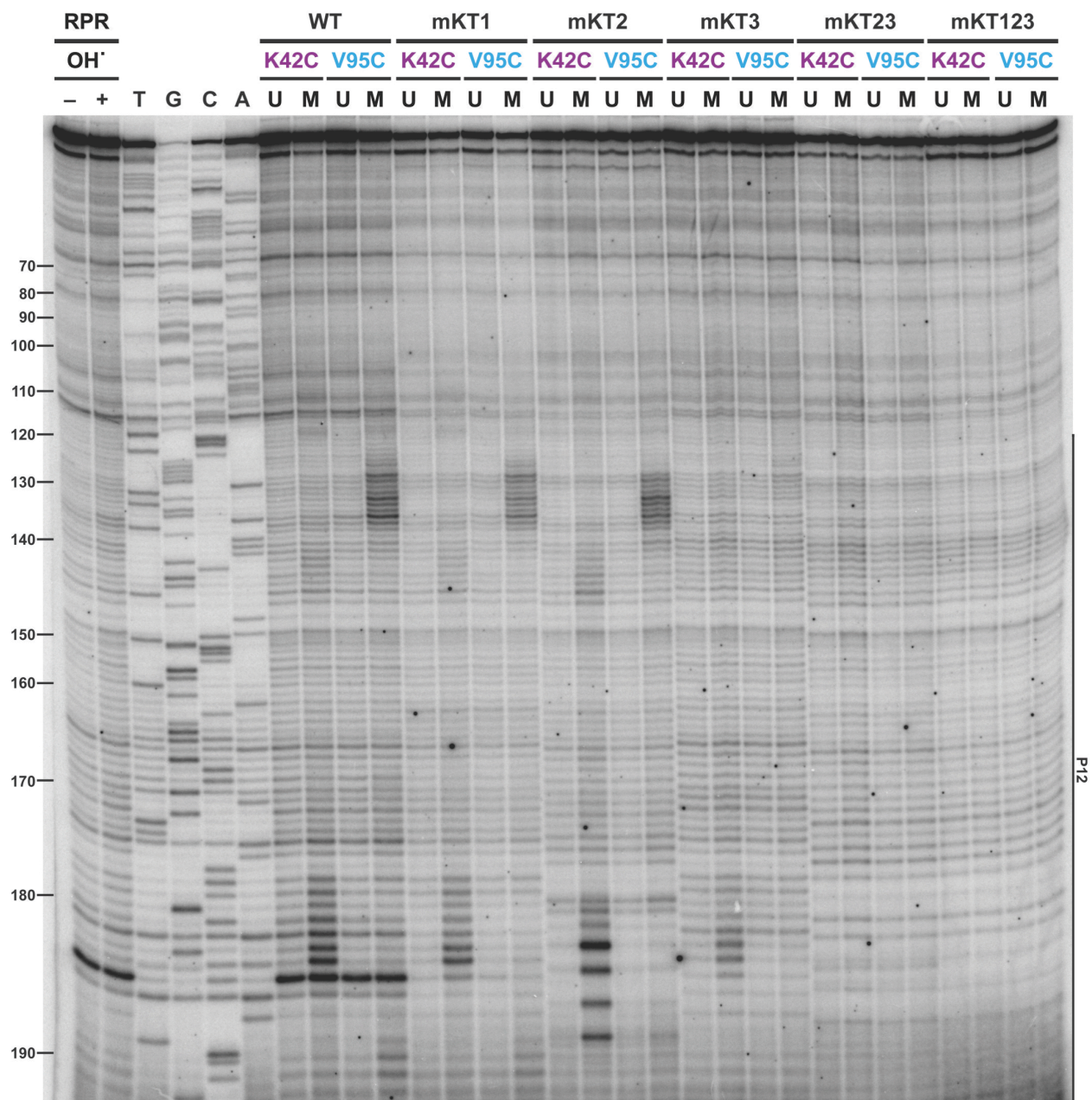
RNA tested	Variable	RPR	RPR-L7Ae ₁	RPR-L7Ae ₂	RPR-L7Ae ₃
	z	16, 17,	18, 19, 20, 21	20, 21, 22, 23	22, 23, 24, 25
PfuRPR	m	110,211	123,736	137,261	150,786
	σ	286	330	330	330
PfuRPR-mKT1	m	110,163	123,688	137,213	
	σ	242	286	286	
PfuRPR-mKT2	m	110,202	123,727	137,252	
	σ	286	330	330	
PfuRPR-mKT3	m	110,163	123,688	137,213	
	σ	286	330	330	
PfuRPR-mKT23	m	119,154	123,679		
	σ	264	308		
PfuRPR-mKT123	m	110,106			
	σ	264			

Because of 3' heterogeneity in the RPR, three major RPR lengths (n , $n+1$, and $n+2$) were considered in our simulation. We used four simulations for $n+1$ [305 (C), 306 (U), 329 (A), 345 (G)] and ten simulations for $n+2$ [610 (CC), 611 (CU), 634 (CA), 650 (CG), 612 (UU), 635 (UA), 651 (UG), 658 (AA), 674 (AG) and 690(GG)]. Assuming all four nucleotides have an equal probability for being incorporated during non-templated 3' additions, h for each was assigned the same value within the simulation. While the ratio

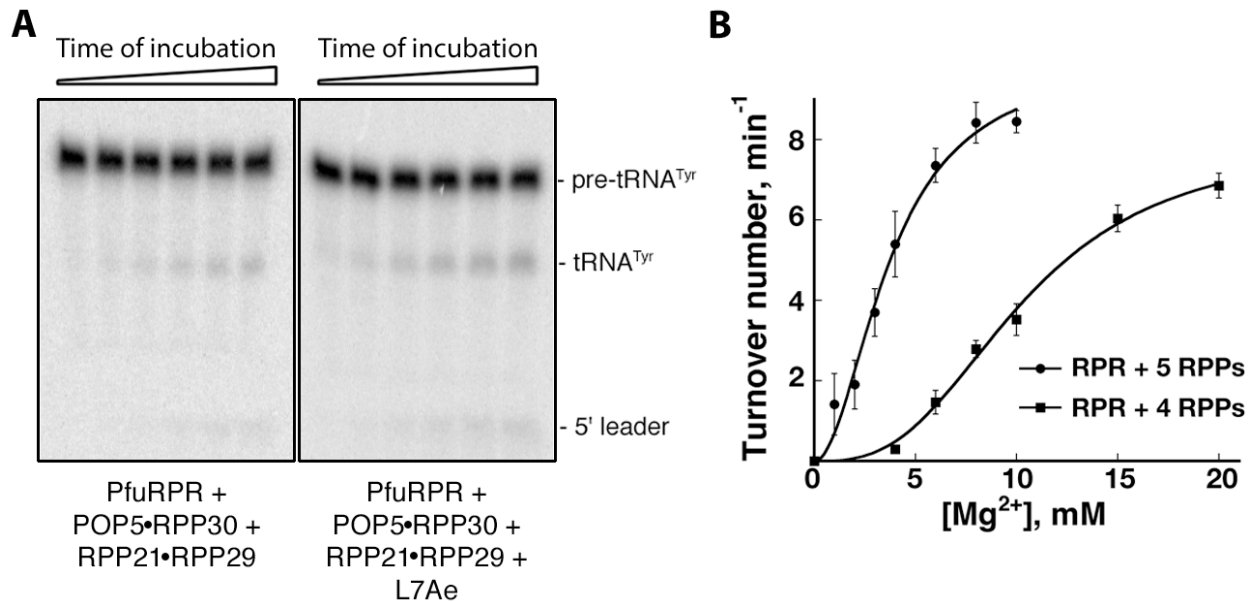
of h between n , $n+1$, and $n+2$ were kept constant in each analysis, the absolute h for each charge state group (e.g., PfuRPR with 17 charges has a different height than PfuRPR with 18 charges) was estimated by coarsely fitting the integration of all simulations (red dotted line) to the experimental (black solid line).



Supplementary Figure S3. Gel-shift analysis of L7Ae binding to a P12 fragment of PfuRPR. The 43-nt PfuP12 fragment consists of a portion of P12a, the double K-turn, P12b, and terminates with a non-native GAAA tetraloop. PfuL7Ae (0-10 μ M) was titrated with a trace amount of 5'-radiolabeled PfuP12. While two complexes were formed with the wild-type (WT) RNA, mutation of either KT2 or KT3 eliminated the higher-order complex. Nucleotide numbering is the same as that used for the full-length PfuRPR.



Supplementary Figure S4. A closer examination of the PfuL7Ae footprint in the double K-turn of PfuRPR and its mutant derivatives. The RNA cleavage products were reverse transcribed using 5'-radiolabeled PfuRPR-2R (Supplementary Table S2). U, unmodified; M, EDTA-Fe-modified.



Supplementary Figure S5. L7Ae decreases the Mg²⁺ dependence of *Pfu* RNase P. **(A)** Representative gels that depict the pre-tRNA processing activity of *Pfu* RNase P reconstituted with RPR + 4 RPPs (left) and with RPR + 4 RPPs + L7Ae (right). These data represent activity assays performed at 8 mM MgCl₂, with aliquots withdrawn at 10-s intervals. **(B)** Plot of turnover number versus [Mg²⁺] for the two complexes. Mean and standard deviation values were calculated from three independent measurements.